Catal Lett (2009) 129:394–399
DOI 10.1007/s10562-009-9845-x

Effect of the Preparation Conditions of Ru/CeO_2 Catalysts for the Liquid Phase Oxidation of Benzyl Alcohol

Saburo Hosokawa · Yukihiro Hayashi · Seiichiro Imamura · Kenji Wada · Masashi Inoue

Received: 5 January 2009 / Accepted: 5 January 2009 / Published online: 17 January 2009

Abstract Ceria colloidal particles with a mean crystallite size of 2 nm were synthesized by a solvothermal reaction. The Ru/CeO_2 catalyst prepared from the CeO_2 colloids exhibited higher activity than the catalyst prepared from $Ce(NO_3)_3$. Temperature-programmed reduction analysis indicated that the reduction of surface Ce^{4+} was accelerated by highly dispersed Ru species on the CeO_2 particles and occurred at low temperatures. The single component CeO_2 sample prepared by the coagulation of the CeO_2 colloid was more easily reduced and re-oxidized than the CeO_2 sample prepared by the precipitation method from $Ce(NO_3)_3$. The higher activity of Ru/CeO_2 prepared from the CeO_2 colloids came from the inherent nature of the CeO_2 support itself.

Keywords CeO_2 · Ru/CeO_2 · CeO_2 nanoparticles · Oxidation · Benzyl alcohol · Solvothermal method

1 Introduction

Ceria is widely used as catalysts or catalyst supports because of its unique functions different from other oxide supports. Ceria is an important oxygen-storage component inevitable for automobile catalysts [1–4], and its high oxygen storage capacity (OSC) is due to a facile shift between Ce^{4+} and Ce^{3+} states under oxidative and reductive conditions [2]. The excellent function of ceria arises when it is combined with noble metals such as Pd, Rh, Pt, and Ru. Ceria prevents the sintering of these noble metals, thus stabilizing their dispersed states [5]. Ceria also stabilizes alumina supports and keeps their high surface areas [6].

Among various noble metal–ceria systems, the Ru/CeO_2 catalyst is known to be remarkably effective for the oxidation of organic pollutants in waste water [7, 8]. It is also active for N_2O decomposition using C_3H_6 as a reductant [9] and the liquid-phase oxidation of alcohols in organic media [10, 11].

Previously, we found that the reaction of rare earth metals such as Ce, Sm and Yb in 2-methoxyethanol at 200–300 °C (solvothermal reaction) yielded transparent colloidal solutions of ultrafine CeO_2, Sm_2O_3, and Yb_2O_3 particles with diameters of 2–3 nm [12]. The pore structure of CeO_2 powders obtained by coagulating the CeO_2 colloidal particles can be controlled by the choice of alkaline coagulant [13]. The CeO_2 obtained by the coagulation with NaOH or $(NH_4)_2CO_3$, followed by calcination at 300 °C, had a large surface area (about 120 m^2/g).

In this work, we tried to prepare a highly active Ru/CeO_2 catalyst utilizing the unique feature of the 2 nm-sized colloidal CeO_2 particles. Five Ru/CeO_2 catalysts were prepared by different methods, and the state of the Ru species on the CeO_2 particles was analyzed in relation to the catalytic activity in the liquid-phase oxidation of benzyl alcohol. The difference in the surface properties of the CeO_2 samples prepared from colloidal CeO_2 and from cerium(III) nitrate was also analyzed.

2 Experimental

2.1 Synthesis of Ceria Colloidal Particles by the Solvothermal Reaction

Cerium metal chips (size, ca. 3.5 × 2.0 × 1.0 mm; total, 5 g) and 2-methoxyethanol (80 mL) were placed in a Pyrex

S. Hosokawa · Y. Hayashi · S. Imamura · K. Wada · M. Inoue (✉)
Department of Energy and Hydrocarbon Chemistry, Graduate School of Engineering, Kyoto University, Katsura, Kyoto 615-8510, Japan
e-mail: inoue@scl.kyoto-u.ac.jp

test tube, and the tube was set in an autoclave (200 mL). In the gap between the test tube and the autoclave wall, an additional 40 mL of 2-methoxyethanol was charged. After completely purged with nitrogen, the autoclave was heated to 250 °C at a rate of 2.5 °C/min and kept at that temperature for 2 h. The reaction mixture was centrifuged at 3,000 rpm for 10 min to remove coarse particles originating from the superficial layer of the Ce metal chips; a transparent solution containing CeO_2 colloidal particles was obtained. The ceramic yield of CeO_2 obtained from the solution was about 70% (ca. 4 g).

2.2 Preparation of CeO_2 Powder Samples

Two kinds of single-component CeO_2 powder samples were prepared.

CeO_2-A: To the CeO_2 colloidal solution (100 mL; CeO_2, 3–4 g) synthesized by the solvothermal reaction, 3 M-NaOH (200 mL) was added, and the thus-obtained ceria coagulate was washed with deionized water repeatedly until the pH of the filtrate became lower than 8, and finally with methanol. The products were dried at room temperature overnight, followed by calcination at 400 °C for 3 h in air.

CeO_2-D: To an aqueous solution (500 mL) containing $Ce(NO_3)_3{\cdot}6H_2O$ (0.03 mol; 5.16 g as CeO_2), 3 M-NaOH (200 mL) was added and the precipitate was washed, dried, and calcined under the condition mentioned above.

2.3 Preparation of Ru/CeO_2 Catalysts

Four Ru/CeO_2 catalysts (A–D) were prepared by different methods, three of which (A–C) utilized the ceria colloidal solution synthesized by the solvothermal method. The Ru loading was adjusted to 2 wt% on metal basis.

Catalyst A: To an aqueous solution (500 mL) containing the CeO_2 colloids (in 100 mL of 2-methoxyethanol; CeO_2, 3–4 g), $RuCl_3{\cdot}nH_2O$, and formalin (10 mL), 3 M NaOH was added until the pH of the solution became about 11. The thus-obtained precursor solid was washed with deionized water until the pH of the filtrate became below 8, and it was calcined at 500 °C for 3 h in air.

A CeO_2 coagulate was used to prepare catalysts B and C. This coagulate was obtained by treating the ceria colloidal solution with 1 M NaOH, followed by washing and calcination at 300 °C.

Catalyst B: The CeO_2 coagulate (1.0 g) was impregnated with a THF solution (15 mL) of ruthenium(III) tris–acetylacetonate (B1), $Ru_3(CO)_{12}$ (B2) or $RuCl_3{\cdot}nH_2O$ (B3). After the solvent was evaporated, the precursor was calcined under the same conditions applied for catalyst A.

Catalyst C: To an aqueous suspension of the CeO_2 coagulate (3 g) containing $RuCl_3{\cdot}nH_2O$ and formalin (10 mL), 3 M NaOH was added up to pH = 11, and the precursor solid thus obtained was washed and calcined just as for catalyst A.

Catalyst D: To an aqueous solution (500 mL) containing $Ce(NO_3)_3{\cdot}6H_2O$ (0.03 mol,: 5.16 g as CeO_2), $RuCl_3{\cdot}nH_2O$ and formalin (10 mL), 3 M NaOH was added up to pH = 11, and the precursor solid obtained was washed and calcined as described above.

2.4 Liquid Phase Oxidation of Benzyl Alcohol

The catalyst (0.5 g, Ru: 0.1 mmol), acetonitrile (10 mL), and benzyl alcohol (1 mmol in 5 mL of acetonitrile) were charged in a glass vessel equipped with a reflux condenser. The vessel was immersed in an oil bath maintained at 50 °C and the mixture was stirred with a magnetic agitator under atmospheric O_2. Benzyl alcohol conversion and benzaldehyde yield were determined after 4 h reaction with a FID gas chromatograph (Shimadzu GC-14A) using diphenyl ether as an internal standard.

2.5 Characterization

The XRD analysis was performed with a Shimadzu XD-D1 X-ray diffractometer. The crystallite size of ceria was calculated from the 220 diffraction peak (47.5° 2θ) based on the Scherrer equation.

The TPR was carried out with a flow-type reactor under the atmospheric pressure. Hydrogen (2 vol% in Ar; 30 mL/min) was passed through a quartz tube containing the sample. The sample tube was heated with an electric furnace, and the amount of H_2 consumed was monitored with a TCD detector of a gas chromatograph (Shimadzu 4CPT).

Nitrogen adsorption isotherms were measured using a volumetric gas-sorption system (Quantachrome Autosorb-1).

3 Results and Discussion

3.1 Oxidation Activity and Characteristics of Ru/CeO_2 Catalyst

Catalysts A and B1 prepared from the ceria obtained by the solvothermal method showed higher activities than catalyst D prepared by the conventional precipitation method (Table 1). Although the BET surface area of catalyst B1 was lower than that of catalyst A, their performances were essentially the same. The BET surface area of catalyst C was much lower than that of catalyst D; however, these two catalysts gave essentially the same benzaldehyde yield. The oxidation activity of the Ru/CeO_2 catalysts, therefore, is not sensitive to their BET surface areas.

Figure 1 shows the XRD patterns of the catalysts. All the diffraction peaks detected for the catalysts A, B1 and D are attributed to CeO_2, suggesting that the Ru species were highly dispersed on the CeO_2. On the other hand, catalyst C exhibited a peak due to RuO_2 ($2\theta = 35^\circ$); a part of the Ru species was crystallized.

The TPR measurement was carried out to see the reduction behavior of Ru/CeO_2 (Fig. 2). Catalysts A, B1 and D had only one reduction peak at around 75 °C, while catalyst C exhibited two peaks at 75 and 85 °C. Previously, we reported that the Ru species on CeO_2 have two reduction peaks; the low-temperature peak is attributed to the reduction of highly dispersed Ru species, and the high-temperature peak is due to the reduction of bulk RuO_2 [14]. Figure 2 indicates that catalysts A, B1, and D have only highly dispersed Ru species, while catalyst C has both highly dispersed Ru species and bulk RuO_2. This result accords with the XRD results.

In the previous work, we found that the active sites of the Ru/CeO_2 catalyst for benzyl alcohol oxidation are highly dispersed Ru species [13], which have a pentacoordinated structure formed from Ru–O–Ce and Ru = O bonds [9]. Judging from the XRD analysis and TPR measurement, the benzaldehyde yields of catalysts A, B1 and C can correlate to the amount of the highly dispersed Ru species on CeO_2.

Catalysts B and C were prepared from the CeO_2 coagulate. Although this sample had both micro- and mesopores, it possessed a large pore volume due to micropores as judged by the N_2 adsorption isotherm (Fig. 3). We found that only a small amount of the Ru species is loaded on the surface inside the micropores of CeO_2 coagulates by the formalin reduction method [13] presumably because the Ru metal particles formed by the reduction of Ru precursor with formalin cannot penetrate into the micropores through the narrow entrance of the pores. Therefore, a large part of the Ru species in catalyst C was loaded on the outer surface of CeO_2 coagulates, making RuO_2 particles grow large on calcination. On the other hand, catalyst B was prepared using a THF solution of a Ru compound that could diffuse into the micropores of CeO_2 coagulates, and Ru species were, therefore, highly dispersed inside the micropores of CeO_2 coagulates.

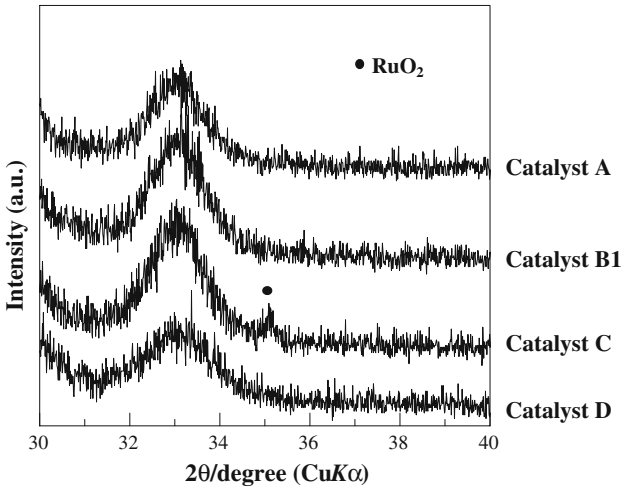

Fig. 1 XRD patterns of Ru/CeO_2 catalysts prepared by various methods

The activity (benzaldehyde yield: 61%) of the catalyst B2 was almost the same as catalyst B1. However, the activity of catalyst B3 was low (benzaldehyde yield: 22%), suggesting that chloride ions remaining in the catalyst retarded the reaction.

In the process of preparing catalyst A, coagulation of ceria colloid, precipitation of Ru species and reduction of Ru by formalin take place simultaneously. In other words, Ru loading and pore formation occur at the same time. Therefore, Ru species can be loaded even on the surface inside the micropores, leading to the high activity of this catalyst.

Table 1 BET surface area, H_2 consumption and oxidation activity of Ru/CeO_2

Method[a]	Ce source	Ru source	BET surface area (m^2/g)	H_2 consumption[b] ($\times 10^4$ mol/g)	Benzyl alcohol conservation[c] (%)	Benzaldehyde	
						Selectivity[c] (%)	Yield[c] (%)
A	Ce colloid	$RuCl_3 \cdot nH_2O$	135	8.7	78	79	60
B1	Ce coagulate	$Ru(acac)_3$	106	7.8	70	85	60
B2	Ce coagulate	$Ru_3(CO)_{12}$	–	–	67	91	61
B3	Ce coagulate	$RuCl_3 \cdot nH_2O$	–	–	33	67	22
C	Ce coagulate	$RuCl_3 \cdot nH_2O$	80	7.3 (5.6)[d]	42	88	37
D	$Ce(NO_3)_3 \cdot 6H_2O$	$RuCl_3 \cdot nH_2O$	142	7.2	53	67	36

[a] See the text

[b] Theoretical H_2 consumption based on the reduction, $RuO_2 + H_2 \rightarrow Ru^0 + 2H_2O$, is 4.0×10^{-4} mol/g

[c] After 4 h

[d] H_2 consumption was calculated from the peak at low temperature range from 60 to 85 °C

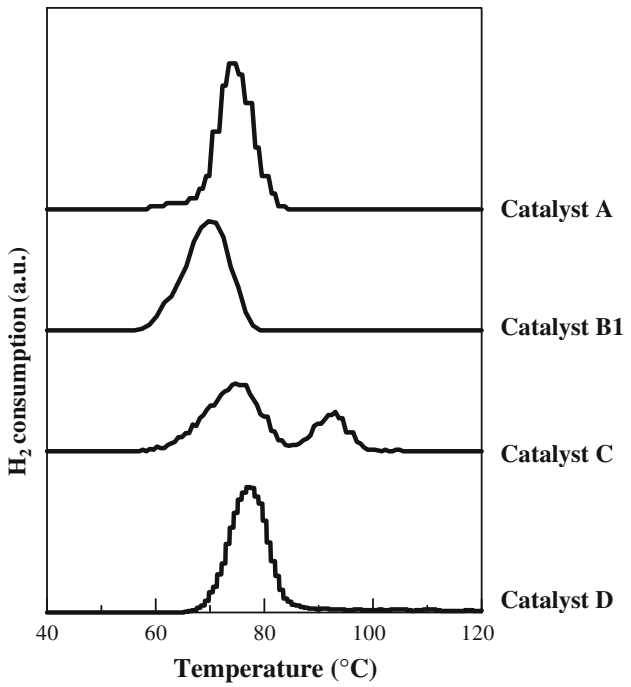

Fig. 2 TPR of Ru/CeO_2 catalysts prepared by various methods. Heating rate, 2 °C/min; Catalyst loading, 0.05 g; 2% of H_2 in Ar (30 mL/min)

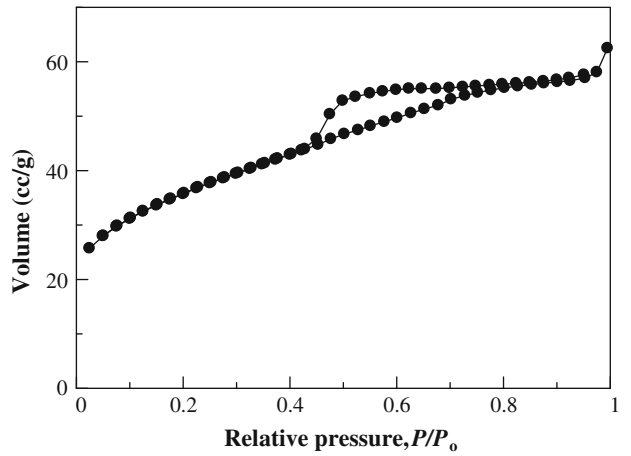

Fig. 3 N_2 adsorption isotherm of CeO_2 coagulate obtained by coagulation of CeO_2 colloid with 1 M NaOH

3.2 Reduction Behavior of Ru/CeO_2 Catalyst

Table 1 also shows the amount of H_2 consumed on the Ru/CeO_2 catalysts (Fig. 2). The theoretical hydrogen consumption is calculated on the basis of the following equation, assuming that all of the Ru species are in the form of RuO_2:

$$RuO_2 + 2H_2 \rightarrow Ru^0 + 2H_2O$$

The amounts of H_2 consumed on all the Ru/CeO_2 catalysts were much larger than the theoretical value (4.0×10^{-4} mol/g), indicating that the reduction of the CeO_2 occurred in addition to the reduction of the Ru species.

Figure 4 shows the TPR profiles for catalyst D, RuO_2 mixed with α-alumina, and CeO_2-D. Two reduction peaks appeared for pure CeO_2. The low-temperature peak observed at around 400 °C is attributed to the reduction of the surface Ce species in a valence state of four, and the peak at higher temperature is ascribed to the reduction of lattice Ce^{4+} [2]. On Ru loading, the reduction peak of CeO_2 at lower temperature disappeared. The amount of H_2 consumed by Ru/CeO_2 (Catalyst D, 7.2×10^{-4} mol/g) is essentially the same as the total amount of H_2 consumed by RuO_2/α-alumina (2.7×10^{-4} mol/g) and by the pure CeO_2 sample at low-temperature (4.1×10^{-4} mol/g). These results clearly indicate that the reduction of CeO_2 surface is accelerated by the Ru species loaded on the CeO_2 particles and occurs simultaneously with the reduction of the Ru species.

The acceleration of reduction of CeO_2 surface can be explained either by hydrogen spillover from Ru species to the surface of CeO_2 facilitating the reduction of surface Ce^{4+} or by oxygen migration from CeO_2 to Ru species where the oxygen reacts with hydrogen yielding water.

TPR profiles of catalyst A measured with various heating rates are shown in Fig. 5. The reduction peak of Ru/CeO_2 was observed at 47–60 °C at heating rate of 0.5 °C/min, and was shifted toward higher temperature with the increase in heating rate. These results suggest that the contact time of hydrogen with catalyst affected the reduction temperature. Therefore, we concluded that the oxygen migration is a rather slow process but can contribute to the benzyl alcohol oxidation at 50 °C for 4 h. Note that the apparent intensity of the reduction peak

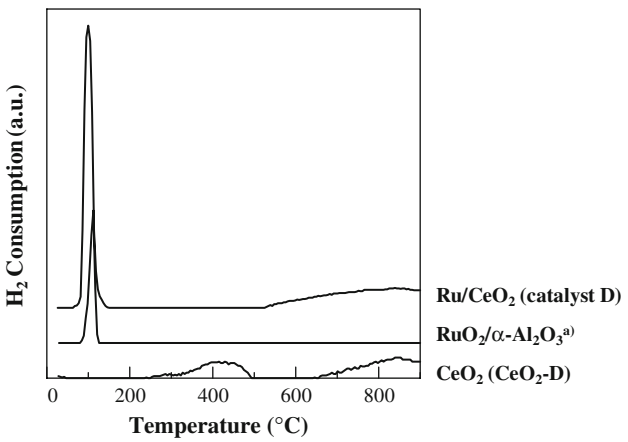

Fig. 4 TPR profiles of Ru/CeO_2 (catalyst D), RuO_2/α-Al_2O_3 (RuO_2 was physically mixed with α-alumina. The Ru content was adjusted to 2 wt% on metal basis) and CeO_2 (CeO_2-D). Heating rate, 5 °C/min; Catalyst loading, 0.1 g; 2% of H_2 in Ar (30 mL/min)

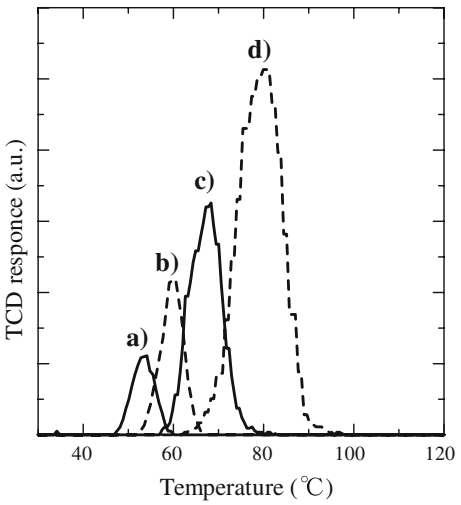

Fig. 5 TPR profiles of Ru/CeO_2 (catalyst A) at various heating rates; (*a*), 0.5 °C/min; (*b*), 1 °C/min; (*c*), 2 °C/min; (*d*), 5 °C/min

decreased with the decrease in the heating rate. This is because the temperature is taken as the abscissa of the figure and total hydrogen consumptions calculated by integration of the TCD response with time were essentially identical for the results with all the heating rates.

3.3 Reduction–oxidation Behavior of CeO_2 Support

Close examination of the data shown in Table 1 revealed that the benzyl alcohol conversion depended on H_2 consumption calculated from the TPR peak observed up to 85 °C. Although catalyst D has highly dispersed Ru species (i.e., the XRD pattern and TPR profile of catalysts D were essentially the same with those of catalyst A). Catalyst D exhibited a low H_2 consumption and a low benzyl alcohol conversion. Since the H_2 consumption calculated from the TPR profile contains the H_2 consumption due to reduction

Table 2 TPR of CeO_2-A and CeO_2-D

	CeO_2 source	BET surface area (m^2/g)	Crystallyte size (nm)	H_2 consumed ($\times 10^{-4}$ mol/g)			Extent of reoxidation[c] (%)
				First run	Second run		
				L[a]	L[a]	H[b]	
CeO_2-A	CeO_2 colloid	103	7.7	3.6	2.9	5.4	81
CeO_2-D	$Ce(NO_3)_3 \cdot 6H_2O$	139	7.4	4.1	2.5	4.3	61

[a] Low temperature peak

[b] High temperature peak

[c] Defined by $(L_{first}/L_{second}) \times 100$. L_{first} and L_{second} are the amounts of H_2 consumed at low temperature region in the first and second runs, respectively

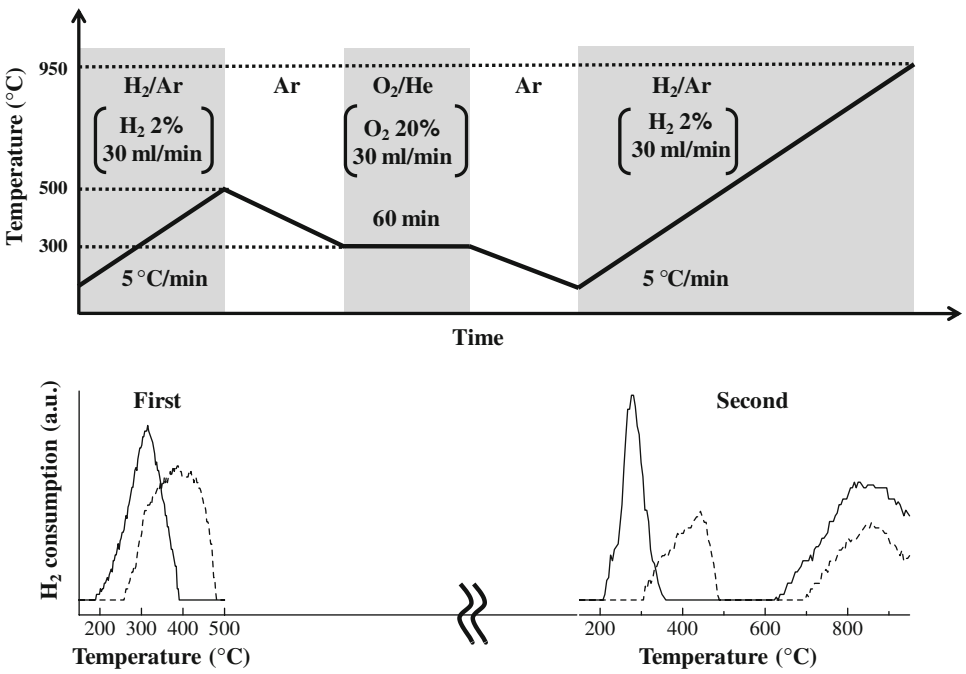

Fig. 6 Repeated TPR analysis of CeO_2-A (*solid line*) and CeO_2-D (*broken line*). Temperature diagram for the experiment is given in the *upper part* of the figure

of CeO_2 surface, inherent nature of CeO_2 particles affects the TPR behavior and thus the catalyst activity: Catalyst A was prepared from the CeO_2 colloids synthesized by the solvothermal reaction of Ce metal, while catalyst D was prepared from $Ce(NO_3)_3$. Therefore, the reduction–oxidation behavior of pure CeO_2 samples prepared from CeO_2 colloids (CeO_2-A) and $Ce(NO_3)_3$ (CeO_2-D) was investigated. Since the BET surface areas of CeO_2 obtained by the calcination at 500 °C (CeO_2-A; 78 m^2/g, CeO_2-D; 111 m^2/g) were smaller than those of the Ru/CeO_2 catalysts, the CeO_2 samples calcined at 400 °C were used in these experiments. The BET surface areas of Ru/CeO_2 catalysts and the CeO_2 samples calcined at 400 °C are shown in Tables 1 and 2, respectively.

In the upper part of Fig. 6, the temperature diagram of the experiment is shown. First, the sample was reduced at a rate of 5 °C/min up to 500 °C, then, oxidized with O_2 (20 vol% in He) at 300 °C for 1 h, and, finally, subjected to the subsequent TPR procedure up to 950 °C. The results are shown in the lower part of Fig. 6. The reduction of surface CeO_2 took place at lower temperature for CeO_2-A than for CeO_2-D, indicating that their surface properties are different. Intensity of the low-temperature peak at the second reduction also differed between CeO_2-A and CeO_2-D: Reduction of the surface of CeO_2-A required a larger amount of H_2 as compared with CeO_2-D (Table 2), indicating that only a part of the surface of CeO_2-D was re-oxidized. Recovery of the oxidized state of the CeO_2 surface on re-oxidation treatment was calculated by comparing the first and the second reduction peaks at low temperature region. For CeO_2-A, 81% of the original oxidized surface was recovered, while only 61% for CeO_2-D. These results indicate that the surface of CeO_2-A prepared from CeO_2 colloids is more easily reduced (lower reduction temperature) and more easily re-oxidized than CeO_2-D. In other words, CeO_2-A prepared from the CeO_2 colloids has high surface oxygen mobility. These results suggest that the high performance of the Ru/CeO_2 catalyst prepared from the solvothermally synthesized CeO_2 colloidal particles is due to the high oxygen mobility of the CeO_2 support.

4 Conclusions

Among the Ru/CeO_2 catalysts prepared from CeO_2 colloids (catalysts A–C), catalysts A and B had higher activity for the oxidation of benzyl alcohol than catalyst C. The TPR and XRD analysis indicated that the Ru species in catalysts A and B were highly dispersed on the CeO_2 particles. The oxidation activity of the Ru/CeO_2 catalysts was sensitive to the dispersion of the Ru species on the CeO_2 particles, but not to the surface area of the catalysts.

Catalyst A prepared from the ceria colloid showed higher activity than catalyst D prepared by a precipitation method. TPR analyses of the CeO_2 supports indicated that CeO_2-A prepared from the CeO_2 colloid was more easily reduced and re-oxidized than CeO_2-D prepared from $Ce(NO_3)_3$. Therefore, the oxygen mobility of the CeO_2 support and the dispersion state of Ru species are the key factors for the oxidation activity of Ru/CeO_2.

References

1. Kim G (1982) Ind Eng Chem Prod Res Dev 21:267
2. Yao HC, Yao YFY (1984) J Catal 86:254
3. Kašpar J, Fornasiero P, Graziani M (1999) Catal Today 50:285
4. Gandhi HS, Graham GW, McCabe RW (2003) J Catal 216:433
5. Cook A, Fitzgerald AG, Cairns JA (1992) In: Dines TJ, Rochester CH, Thomson J (eds) Catalysis and surface characterization. Royal Society of Chemistry, Cambridge, p 249
6. Normand FL, Hilaire L, Kile K, Maire G (1988) J Phys Chem 92:2561
7. Oliviero L, Barbier J Jr, Duprez D, Wahyu H, Ponton JW, Metcalfe IS, Mantzavinos D (2001) Appl Catal B: Environ 35:1
8. Renard B, Barbier J Jr, Duprez D, Durécu S (2005) Appl Catal B: Environ 55:1
9. Hosokawa S, Nogawa S, Taniguchi M, Utani K, Kanai H, Imamura S (2005) Appl Catal A: General 288:67
10. Vocanson F, Guo YP, Namy JL, Kagan HB (1998) Synth Commun 28:2577
11. Ji H, Mizugaki T, Ebitani K, Kaneda K (2002) Tetrahedron Lett 43:7179
12. Kobayashi T, Hosokawa S, Iwamoto S, Inoue M (2006) J Am Ceram Soc 89:1205
13. Hayashi Y, Hosokawa S, Imamura S, Inoue M (2007) J Ceram Soc Jpn 115:592
14. Hosokawa S, Kanai H, Utani K, Taniguchi Y, Saito Y, Imamura S (2003) Appl Catal B: Environ 45:181